JOURNAL OF CATALYSIS 113, 106–119 (1988)

Effects of Dopants on Performance of Metal Crystallites

2. Further Characterization of Doped Supports and Catalysts

EDMOND C. AKUBUIRO AND XENOPHON E. VERYKIOS[1]

Department of Chemical Engineering, Drexel University, Philadelphia, Pennsylvania 19104

Received May 18, 1987; revised March 21, 1988

The effects of dopants on chemisorptive and catalytic properties of metal crystallites are further investigated by additional characterization of supports and catalysts. Alterations of the Fermi energy level of TiO_2 doped with altervalent cations are detected by measurements of specific electrical conductivity and activation energy of electron conduction. It is established that under any environment the specific electrical conductivity of higher-valence doped TiO_2 is significantly higher than that of undoped, equal-, and lower-valence doped TiO_2. The CO chemisorption capacity of Pt supported on higher-valence doped carriers is found to be significantly reduced and to follow the same general trends as those of O_2 and H_2. Shifts in the vibrational frequency of CO adsorbed on these catalysts indicate that the metal–carbon bond is weakened, probably due to increased saturation of Pt *d* orbitals as a result of electronic interactions at the metal–support interface.

INTRODUCTION

The effects of altervalent cation doping of TiO_2 carriers on the chemisorptive properties of small Pt crystallites were discussed in an earlier paper (*1*). Normal chemisorption capacity for H_2 and O_2 was observed on Pt supported on titania doped with lower- and equal-valence cations (K^+, Mg^{2+}, Ge^{4+}), while an irreversibly suppressed chemisorption of these gases was observed on Pt particles supported on titania doped with higher-valence cations (Ta^{5+}, Sb^{5+}, W^{6+}). TEM studies showed that the degrees of dispersion of Pt on doped and undoped carriers were approximately the same, indicating that the observed phenomena are not a consequence of enlargement of Pt crystallites. ESCA results indicated that no segregation of the dopants occurred on the surface of the catalyst carriers, indicating that the observed phenomena cannot be attributed to coverage of the metal surface with the doping cations. The phenomenon of suppressed chemisorption capacity of Pt crystallites supported on higher-valence doped titania was found to be a strong function of the size of the metal particles, its magnitude decreasing significantly at metal crystallites exceeding 40 Å.

These results were interpreted in terms of extended electronic interactions at the metal–semiconductor interface which was viewed as a Schottky junction. The electronic interaction at the metal–semiconductor interface is attributed to the increased Fermi energy level of the higher-valence doped titania carriers. Such interactions alter the electronic structure of Pt by partially saturating its *d* orbitals, allowing it to gradually resemble the d^{10} configuration of its neighbor in the periodic table, gold, which is a poor adsorber of H_2 and O_2. These ideas were first proposed by Schwab (*2*, and references therein) and Solymosi (*3*, and references therein). In a more recent study, Solymosi *et al.* (*4*) demonstrated that Rh crystallites supported on TiO_2 doped with W^{6+}

[1] Present address: Institute of Chemical Engineering and High Temperature Chemical Processes, Department of Chemical Engineering, University of Patras, Patras, Greece.

0021-9517/88 $3.00

ions exhibit enhanced activity in CO and CO_2 hydrogenation and explained this observation with reasoning similar to that described above.

In the present paper we report results of electrical conductivity measurements of doped titania carriers under various environments, which clearly demonstrate that the Fermi energy level of the parent TiO_2 support is significantly altered by altervalent ion doping. The effects of dopants on the chemisorption characteristics of CO on Pt were also investigated in equilibrium chemisorption experiments and in infrared studies of CO adsorbed on Pt supported on doped carriers. These results offer additional, although indirect, evidence of shifts in the electron structure of surface Pt atoms supported on higher-valence doped carriers.

EXPERIMENTAL PROCEDURES

Preparation of doped TiO_2 supports and catalysts was described in a previous paper (*1*). For electrical conductivity measurements, TiO_2 was doped with a lower-valence cation (Mg^{2+}), an equal-valence cation (Ge^{4+}), and higher-valence cations (Ta^{5+}, Sb^{5+}, W^{6+}) in order to alter its electron structure. For ease of reference, samples are indicated as $x\%$ Pt/TiO_2 (*D*), where x designates metal loading and D the dopant.

Electrical conductivity experiments were performed in a flow cell which permits *in situ* studies of changes in electron conduction of a sample under vacuum or in the presence of various gaseous environments. Already powdered samples were further crushed into fines and were compressed into pellets of known dimension (13.5 × 5 mm) by applying a pressure of 800 atm. The conventional, two-probe, direct current technique was employed for all electrical conductivity measurements. Resistances were measured using an EICO Model 950 bridge which has a useful range of 0.1 to 500 MΩ. The bridge was calibrated against precision resistors and found to be within 1% over the range 0.1 to 100 MΩ, and about 5–10% above 100 MΩ. For resistances less than 10^5 Ω, measurements were verified using a Keithley 177 multimeter. Resistances were recorded only when temperature was constant and conductivity did not change with time. Specific electrical conductivities, σ (Ω^{-1} cm^{-1}), were computed from measured conductance ($1/R$), taking into account the geometry of the sample by

$$\sigma = 1/R * t/s, \quad (1)$$

where t is the thickness and s the cross-sectional area of the sample pellet.

Conductivity was measured as a function of temperature under the following atmospheres: (a) vacuum; (b) CO methanation conditions (24% H_2, 8% CO, 68% N_2), which will be referred to as $H_2/CO/N_2$; (c) CO oxidation conditions (4% O_2, 2% CO, 94% N_2), which will be referred to as $O_2/CO/N_2$; (d) CO; and (e) H_2. All measurements, other than vacuum, were conducted at a pressure of 1 atm, in flowing gases. Conductivity measurements were conducted under CO hydrogenation and oxidation conditions because the kinetic parameters of these catalysts were obtained under identical conditions.

Equilibrium adsorption of CO on Pt surfaces was investigated in a constant-volume, high-vacuum apparatus (Micromeritics, Accusorb 2100E). Room-temperature irreversible CO adsorption was measured by extrapolating isotherms to zero pressure. Adsorption on blank supports was accounted for. Pretreatment schedule and other experimental details have been reported elsewhere (*1*). High-purity CO was used in the adsorption experiments and was further purified by being passed through a molecular sieve trap.

For IR studies platinized samples were ground in an agate mortar and sieved (400 mesh) to minimize radiation scattering effects. Catalyst powders were either pressed alone or mixed with TiO_2 before pressing into wafers in a $\frac{1}{2}$-in. die. A pressure of 650 atm was applied to give good mechanical

strength. The wafers were placed in sample holders in portable quartz cells with water-cooled NaCl windows. Cells could be heated to temperatures up to 400°C for pretreatment purposes and they were connected to a gas manifold which permitted *in situ* measurements. Spectra were recorded in a Perkin–Elmer 1800 Fourier transform infrared spectrophotometer equipped with a liquid nitrogen-cooled MCT high-sensitivity detector and a DTGS detector. Several scans were taken to obtain good *S/N* ratio. IR spectra were recorded in the single-beam mode. All samples were given the same pretreatment which consisted of flowing He at room temperature for $\frac{1}{2}$ h, increasing the temperature to 200°C and holding for 1 h, flowing H_2 for 1.5 h, and cooling to room temperature in flowing He. The background spectrum was recorded at this point. Samples were then exposed to flowing CO for a period of approximately 1 h. The gas-phase CO was flushed with He until no gas-phase CO was detected. The background spectrum was subtracted from resulting spectra to obtain the spectrum of adsorbed CO.

RESULTS AND DISCUSSION

(*a*) *Electrical Conductivity Measurements*

The methodology of this investigation involves modification of the electronic structure of TiO_2 by incorporation of altervalent cations into its crystal structure, in order to alter its Fermi energy level. Since measurements of Fermi level or work function of supported metal catalysts can only be achieved with difficulty, electrical conductivity measurements were conducted in order to obtain a qualitative estimate of the extent of modification of the electron state of TiO_2, upon doping. It must also be emphasized that conductivities measured in this study do not indicate absolute, intrinsic values since the samples employed were not single crystals but, rather, powdered and pelletized material.

In addition to specific electrical conductivity measurements, the activation energy of electron conduction, E_C, was also determined. It is well known (*5, 6*) that energetic quantities such as enthalpies of formation of anionic vacancies, energy of electron ionization, or activation energy of electron conduction are not affected by grain boundaries. Hence, E_C constitutes a more reliable means of assessing changes in the electronic state of various samples.

Conductivities measured in this investigation are primarily those of the catalyst carrier since the highly divided state of the metal and its moderate weight percentage do not allow electron conduction through the metal particles (*7*). However, it was deemed necessary to determine the effects of Pt content on overall conductivity. For this purpose the electrical conductivities of Pt/TiO_2, with metal loadings of 0, 0.06, 0.5, and 2%, and of $Pt/TiO_2(Sb^{5+})$ with the same metal loadings were determined in the temperature range 300–600 K, under vacuum and in a reducing atmosphere (24% H_2, in N_2). The effects of temperature on the electrical conductivity of these samples is shown in Fig. 1.

Figure 1 shows that under vacuum, the specific electrical conductivity of platinized TiO_2 decreases with increasing metal loading. Differences in electrical conductivity diminish as temperature increases. This behavior is attributed to an "electron pumping effect" of Pt (*5*). Electrons are being pumped into and tied up at the Pt particles, thereby decreasing the conduction electron density of TiO_2. This effect increases in significance with increasing metal loading, and it is more pronounced at lower temperatures because of the exothermicity of this process (*5*). The observed variation of electrical conductivity with Pt loading under vacuum supports the conclusion that the small amount of metal on the samples does not contribute directly to their conductivity. If that were the case, an enhancement in conductivity would be expected with increasing metal loading since the conductivity of the metal is orders of magnitude higher than that of TiO_2.

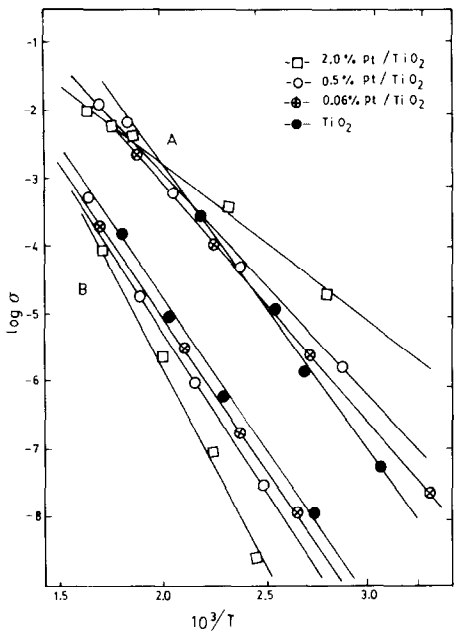

FIG. 1. Effect of temperature on electrical conductivity of Pt/TiO_2 under (A) reducing atmosphere and (B) vacuum.

The variation of electrical conductivity with Pt loading in a reducing atmosphere is the exact opposite of that observed under vacuum. Conductivity is shown to increase with increasing Pt content, especially at low temperatures. This phenomenon is attributed to dissociative adsorption of H_2 on Pt particles and spillover of adsorbed atomic hydrogen to the support, resulting in generation of free electrons. This process increases in significance with increasing Pt loading, thus the observed behavior. The process of electron transfer into Pt particles, which was described earlier, is also present in a reducing environment, but the hydrogen spillover process dominates and the net result is increased concentration of conduction electrons in TiO_2. The adsorption of H_2 on Pt decreases with increasing temperature. As a result, at high temperatures, electrical conductivities seem to merge or to follow the trend observed under vacuum. Thus, the relative significance of the two processes, which affect the concentration of free electrons in TiO_2, seems to be a function of temperature. Identical effects of Pt loading on electrical conductivity were observed on Sb^{5+}-doped TiO_2 samples under vacuum and in the same reducing atmosphere.

The 0.5% Pt catalysts were used in all subsequent electrical conductivity measurements, because the dopant effects were observed to be more pronounced on such samples. Thus, any measured alteration in electrical properties of these samples yields the effective electronic interaction between the supported metal particles and the doped carriers more realistically. To determine if the modification of TiO_2 supports by altervalent ion doping alters the electrical conductivity of TiO_2, conductivity measurements of all doped and undoped samples were conducted in various environments—vacuum, H_2, $H_2/CO/N_2$, $O_2/CO/N_2$, and CO. The effects of dopants on the electrical conductivity and activation energy of electron conduction of TiO_2 under vacuum at 333 K are shown in Fig. 2. It is apparent that under these conditions, the electrical conductivity of titania doped with cations of higher valence (Ta^{5+}, Sb^{5+}, W^{6+}) is two to three orders of magnitude higher than

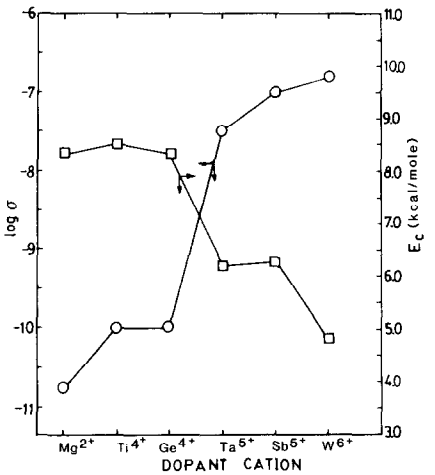

FIG. 2. Effects of dopants on specific electrical conductivity and activation energy of electron conduction of 0.5% Pt/TiO_2 (*D*) at 333 K under vacuum.

TABLE 1

Specific Electrical Conductivity of 0.5% Pt/TiO_2 (*D*) at 450 K in Various Environments

Sample	σ (Ω^{-1} cm^{-1})				
	Vacuum $\times 10^7$	H_2 $\times 10^4$	$H_2/CO/N_2$ $\times 10^5$	CO $\times 10^5$	$O_2/CO/N_2$ $\times 10^{11}$
TiO_2 (Mg^{2+})	0.3	0.4	2	0.6	8
TiO_2	3	8	18	5	6
TiO_2 (s)[a]	2	8	11	3	—
TiO_2 (Ge^{4+})	2	7	12	4	—
TiO_2 (Ta^{5+})	18	12	25	10	40
TiO_2 (Sb^{5+})	22	45	99	50	70
TiO_2 (W^{6+})	18	32	98	40	71

[a] Sample sintered at 900°C for 5 h.

that of undoped titania, while the electrical conductivity of Mg^{2+}-doped TiO_2 is one order of magnitude lower. The conductivity of Ge^{4+}-doped TiO_2 is approximately the same as that of the undoped sample. The activation energy of electron conduction is nearly unaffected by doping with lower- or equal-valence cations, but it is significantly reduced, by approximately 30 to 45%, upon doping with higher-valence cations. Similar results, obtained at 450 K under various environments, are presented in Tables 1 and 2. Although the trends depicted in Fig. 2 are still apparent, the effects of dopants are not as pronounced at the higher temperature. It can also be observed in Tables 1 and 2 that specific electrical conductivity and activation energy are strong functions of the environment under which measurements are conducted.

Based on these results, it can be argued that the conductivity of TiO_2 is significantly affected by the incorporation of cations of different valence into its crystal structure. Nevertheless, the true effect of modification of electronic structure of TiO_2 by altervalent ion doping is given by the activation energy of electron conduction, E_C, which is not influenced by grain boundary effects. The effect of various dopants on the activation energy of electron conduction, E_C, is shown graphically in Fig. 2 for experiments conducted under vacuum. It can be seen that the activation energy of electron conduction of TiO_2 is decreased by 30–45% when titania is doped with cations of higher valence (Ta^{5+}, Sb^{5+}, W^{6+}), whereas no significant change is observed for lower-valence (Mg^{2+}) or equal-valence (Ge^{4+}) doped TiO_2. In any environment—vacuum, H_2, CO, $H_2/CO/N_2$, or $O_2/CO/N_2$—the activation energy of electron conduction, as shown in Table 2, increases in the order TiO_2 (W^{6+}) < TiO_2 (Sb^{5+}) ≈ TiO_2 (Ta^{5+}) < TiO_2 (Ge^{4+}) ≈ TiO_2 (Mg^{2+}) < TiO_2. The greater number of electrons available in a hexavalent-doped TiO_2, compared to a pentavalent-doped TiO_2, is reflected in the lower E_C of the former. The E_C for Ge^{4+}-doped TiO_2 and that of the undoped, sintered titania, TiO_2 (s), are equal due to the fact that doping with Ge^{4+} did not alter the electronic structure of TiO_2. TiO_2 (s) and the doped titania were shown by X-ray diffraction to have undergone extensive rutilization compared to the unsintered TiO_2. Titania with predominantly rutile structure has slightly a higher electron density than that with predominantly anatase structure, probably due to the greater amount of disorders associated with the rutile structure. This translates into a slightly lower E_C of TiO_2 (s) than that of unsintered TiO_2.

TABLE 2

Activation Energy of Electron Conduction of 0.5% Pt/TiO_2 (*D*) in Various Environments

Sample	E_c kcal/mole (eV)				
	Vacuum	H_2	$H_2/CO/N_2$	CO	$O_2/CO/N_2$
TiO_2 (Mg^{2+})	8.3 (0.35)	6.2 (0.26)	6.5 (0.28)	7.0 (0.30)	8.6 (0.36)
TiO_2	9.9 (0.42)	7.4 (0.31)	7.4 (0.31)	7.5 (0.32)	8.2 (0.35)
TiO_2 (s)[a]	8.5 (0.36)	5.9 (0.25)	6.1 (0.26)	6.8 (0.29)	—
TiO_2 (Ge^{4+})	8.3 (0.35)	6.0 (0.25)	6.2 (0.26)	6.6 (0.28)	—
TiO_2 (Ta^{5+})	6.2 (0.26)	4.6 (0.20)	4.7 (0.20)	5.2 (0.22)	6.8 (0.29)
TiO_2 (Sb^{5+})	6.3 (0.27)	4.4 (0.19)	4.8 (0.20)	5.1 (0.22)	7.1 (0.30)
TiO_2 (W^{6+})	4.8 (0.20)	3.0 (0.13)	3.0 (0.13)	3.3 (0.14)	5.6 (0.24)

[a] Sample sintered at 900°C for 5 h.

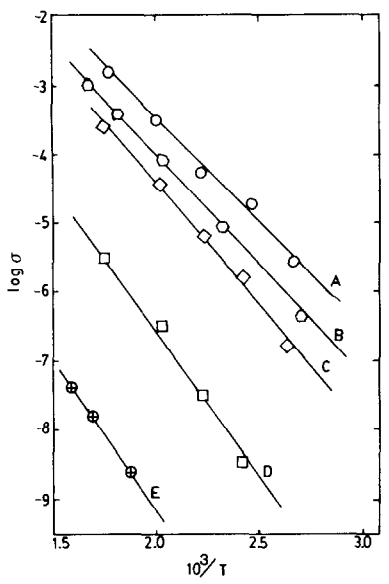

FIG. 3. Temperature sensitivity of electrical conductivity of 0.5% Pt/TiO_2 (Sb^{5+}) (A) in H_2, (B) in $H_2/CO/N_2$, (C) in CO, (D) under vacuum, (E) in $O_2/CO/N_2$.

Representative results indicating the effects of environment on electrical conductivity and activation energy of electron conduction are shown in Fig. 3 for Sb^{5+}-doped catalysts, in the form of Arrhenius plots. Results obtained at 450 K are summarized in Tables 1 and 2. It is apparent that electrical conductivity, and to a smaller extent activation energy, are affected by the environment in which the sample exists. The variation of electrical conductivity with the atmosphere with which the sample is at equilibrium has been discussed by Herrmann and Pitchat (*5*, *7*) and Solymosi (*6*) in terms of dehydration of TiO_2 and subsequent generation of doubly charged oxygen vacancies, loss of lattice oxygen creating anionic vacancies, reaction of CO with lattice oxygen, and hydrogen spillover. The same reasoning can be applied to explain the results shown in Fig. 3 and Tables 1 and 2. Figure 3 and Tables 1 and 2 indicate that, for all samples, specific electrical conductivity and activation energy of electron conduction in various environments decrease in the order $H_2 > H_2/CO/N_2 > CO >$ vacuum $> O_2/CO/N_2$, and conductivity increases with increasing temperature. Using the data obtained from experiments under vacuum as a reference, the conductivity of all samples under reducing conditions is about three orders of magnitude higher than that under vacuum, while the conductivity in an oxidizing atmosphere is about four orders of magnitude lower than that under vacuum. The conductivity of TiO_2 (doped and undoped) is inhibited by oxygen pressure, consistent with the behavior of *n*-type semiconductors. The high conductivity and low activation energy associated with H_2 arise from dehydration of titania and generation of oxygen vacancies and free electrons, while that of CO is a consequence of reaction of CO with lattice oxygen producing CO_2 and free electrons. The low conductivity and high activation energy in an oxygen atmosphere result from the interaction of oxygen with anionic vacancies and free electrons to create lattice oxygen. The constancy of activation energy of electron conduction, or linearity of Arrhenius plots, for all catalyst samples subjected to these conditions indicates that within the temperature range employed in this study, and under conditions employed, the catalyst carriers conserve their semiconducting character.

(*b*) *Equilibrium Adsorption of CO*

The effects of dopants on the chemisorption characteristics of CO on Pt were investigated at room temperature using two sets of catalysts with metal loadings of 0.5 and 2.0%. Typical adsorption isotherms are shown in Fig. 4 and results are summarized in Table 3. The effects of dopants on the chemisorptive capacity of the catalysts is presented in the form of normalized ratios or "suppression factor." The suppression factor is defined as the ratio of the amount of CO adsorbed per Pt atom on the doped samples to the amount adsorbed per Pt atom on the undoped sample. Figure 4 and Table 3 indicate that Pt supported on higher-valence (Sb^{5+}, Ta^{5+}) doped TiO_2 ex-

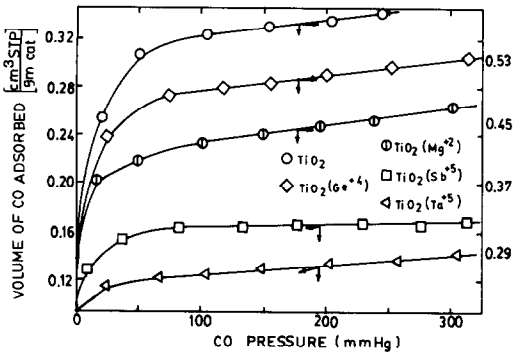

FIG. 4. CO adsorption isotherms of 0.5% Pt/TiO_2 (*D*) at ambient temperature.

TABLE 3

CO Adsorption on Pt/TiO_2 (*D*)

Carrier	Red. Temp. (°C)	0.5% Pt/TiO_2 (*D*)		2% Pt/TiO_2 (*D*)	
		CO/M	$\frac{(CO/M)_d}{(CO/M)_{und}}$	CO/M	$\frac{(CO/M)_d}{(CO/M)_{und}}$
TiO_2	200	0.92	1.00	0.19	1.00
TiO_2 (Mg^{2+})	200	0.69	0.75	0.15	0.78
TiO_2 (Ge^{4+})	200	0.83	0.91	0.16	0.83
TiO_2 (Sb^{5+})	200	0.28	0.30	0.12	0.63
TiO_2 (Ta^{5+})	200	0.23	0.25	0.10	0.52

hibits suppressed CO chemisorption capacity, while Pt supported on lower- and equal-valence (Mg^{2+}, Ge^{4+}) doped TiO_2 exhibits normal CO chemisorption capacity. Table 3 also indicates that the effect of dopants is significantly more pronounced in the 0.5% Pt series than in the 2.0% Pt series. Identical results were obtained in H_2 and O_2 adsorption on these catalysts (*1*). These results were interpreted in terms of long-range electronic interactions between the doped catalyst carriers and the supported metal particles. Thus, these electronic interactions at the metal–semiconductor interface affect the chemisorption characteristics of CO on Pt/TiO_2 (*D*) in a manner identical to that of H_2 and O_2. Detailed discussion of this phenomenon was presented in an earlier publication (*1*).

(*c*) *FTIR Studies of Adsorbed CO*

FTIR spectra of CO adsorbed on Pt/TiO_2 are shown in Figs. 5–7 along with a spectrum of CO adsorbed on Pt/Al_2O_3 for comparative purposes. Results are summarized in Table 4. In most cases, CO adsorbed on freshly reduced Pt surfaces produced three bands in the IR spectrum. A broadband appears below 2000 cm^{-1} (between 1780 and 1860 cm^{-1}). The major band appears between 2050 and 2080 cm^{-1} with a second one which looks like a satellite/shoulder appearing between 2080 and 2095 cm^{-1}. A shift of the major band toward higher frequencies (blue shift) is observed in the vibrational frequency of CO adsorbed on Pt

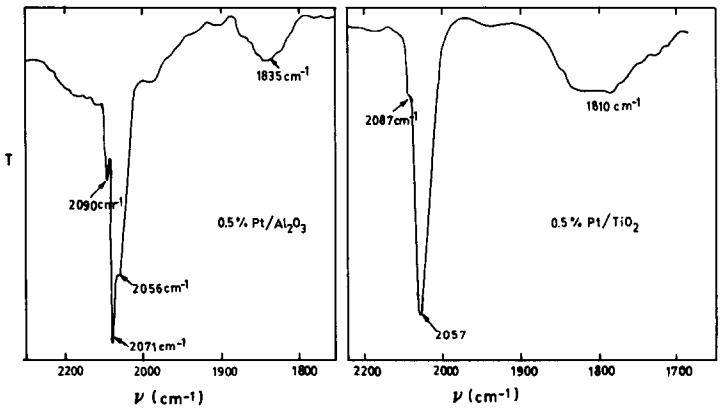

FIG. 5. Infrared spectra of CO adsorbed on 0.5% Pt/Al_2O_3 and 0.5% Pt/TiO_2 at 298 K.

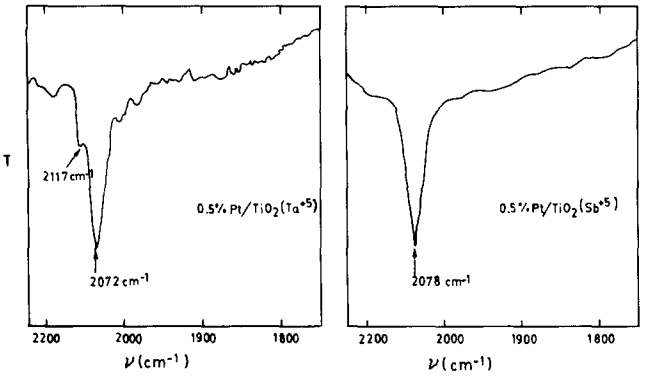

FIG. 6. Infrared spectra of CO adsorbed on 0.5% Pt/TiO_2 (Ta^{5+}) and 0.5% Pt/TiO_2 (Sb^{5+}) at 298 K.

supported on TiO_2 doped with higher-valence cations (Ta^{5+}, Sb^{5+}, W^{6+}) as can be seen in Figs. 6 and 7. This shift is a function of metal loading or metal crystallite size of the catalysts. Thus in the 0.5% Pt catalysts [average crystallite size approximately 20 Å (*1*)] an increase in frequency in the range 15–22 cm^{-1} is observed while in the 2% Pt catalysts [average crystallite size in the range 40–60 Å (*1*)] the frequency shift is only 7–8 cm^{-1}. It must be stated at this point that the instrument resolution was set at 2 cm^{-1}. No significant shift in wavenumbers is observed for Pt supported on lower-valence doped TiO_2. The broadbands which appear around 1830 cm^{-1} did not appear in the higher-valence doped catalysts probably due to suppressed CO adsorption capacity of these catalysts.

The broadband which appears between 1780 and 1860 cm^{-1} is assigned to multicoordinated CO, or more specifically to bridge-bonded CO on two Pt sites (*9–11*). Since this band is weak, it was predominantly seen on catalysts which did not exhibit suppression of CO adsorption. This interpretation is consistent with the results of Ibach *et al.* (*12, 13*) who showed that on clean Pt surfaces linearly bonded CO species appear first and that bridge-bonded CO appears only after 30% or more CO coverage is attained. The major peak which appears between 2050 and 2080 cm^{-1} is generally assigned to linearly

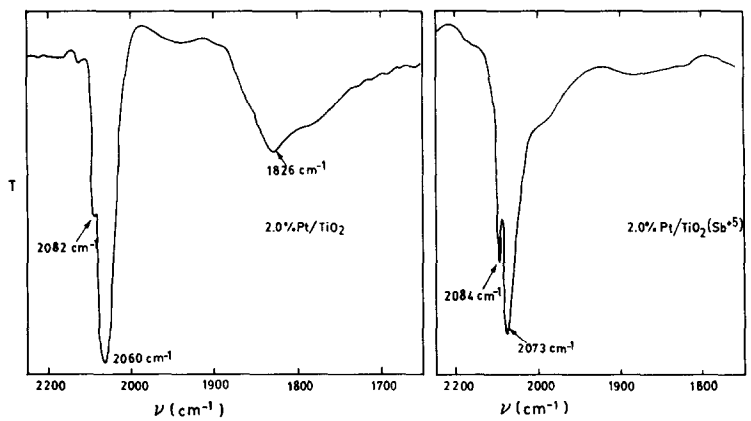

FIG. 7. Infrared spectra of CO adsorbed on 2% Pt/TiO_2 and 2% Pt/TiO_2 (Sb^{5+}) at 298 K.

TABLE 4

Adsorbed CO Band Frequencies at 298 K, for Pt Supported on Doped and Undoped Samples

Catalyst	Observed frequencies (cm^{-1})		
	Major	Minor	
0.5% Pt/TiO_2	2057	2087(s)[a]	1810(b)[a]
0.5% Pt/TiO_2 (Mg^{2+})	2055	2100, 2122	1824
0.5% Pt/TiO_2 (Zn^{2+})	2055	2102	—
0.5% Pt/TiO_2 (Ta^{5+})	2072	2117	—
0.5% Pt/TiO_2 (Sb^{5+})	2078	—	—
0.5% Pt/TiO_2 (W^{6+})	2079	2128	1830(b)
2.0% Pt/TiO_2	2060	2082	1826(b)
2.0% Pt/TiO_2 (Sb^{5+})	2073	2084	—
0.5% Pt/Al_2O_3	2071	2090 2056(s)[a]	1835(b)[b]

[a] (s), shoulder.
[b] (b), broadband.

bonded CO on reduced Pt surfaces. The initial assignment of the HF peak to linearly adsorbed CO and the LF band to bridge-bonded CO was based on metal carbonyl spectra; nevertheless, more direct studies have proven these assignments to be correct (*12*). The HF band has always been reported (*9, 14, 15*) to be more intense than the LF one, in agreement with results obtained in this study. Other adsorption bands observed between 2080 and 2095 cm^{-1} or between 2100 and 2130 cm^{-1} have been assigned to a CO molecule and an oxygen atom bonded to the same Pt site (*15–17*) or to small CO islands completely surrounded by a layer of oxygen atoms (*10, 16*), or to subcarbonyl formation on small metal crystallites (*9, 18, 19*). However, since all catalysts in this study were reduced *in situ* in H_2 at 200°C prior to CO adsorption, the inclination is to attribute the presence of these bands to formation of subcarbonyls on small Pt crystallites.

The reliability of FTIR measurements is determined by comparison of spectra obtained in this study with those reported in the literature. For this reason a spectrum of CO adsorbed on platinized Al_2O_3 was recorded. The major peak observed for linearly bonded CO on 0.5% Pt/Al_2O_3 at 2071 cm^{-1} is in good agreement with values of 2070 to 2073 cm^{-1} reported in the literature for catalysts of approximately the same Pt dispersion (*9, 10, 15, 20*). For 0.5% Pt/TiO_2, the main peak observed at 2057 cm^{-1} fairly conforms with a value of 2050 cm^{-1} reported by Vannice *et al.* (*9*) for 2% Pt/TiO_2.

A shift toward higher frequencies (blue shift) is observed in the vibrational frequencies of CO adsorbed on Pt supported on TiO_2 doped with higher-valence cations (Ta^{5+}, Sb^{5+}, W^{6+}) whereas no significant shift is observed on Pt supported on lower-valence doped TiO_2. Before attempting to link this behavior to electronic interactions, it is necessary to discuss the effects of metal particle size and surface coverage on the frequency of CO adsorption band. It has been shown by many researchers (*10, 14, 20–22*) that a band shift to higher frequency occurs with increasing CO surface coverage. A similar observation has been made by Barth *et al.* (*23*) in our laboratory. Since the higher-valence doped catalysts exhibit reduced CO chemisorption capacity (Table 4), a shift in the opposite direction (lower frequencies) would be expected as a result of reduced surface coverage. Barth *et al.* (*23*) have also found no substantial shift over a wide dispersion of Pt on TiO_2. It can be concluded, therefore, that metal particle size and CO surface coverage are not responsible for the blue shift exhibited by higher-valence doped catalysts.

Any modification in the metal–adsorbate bond strength affects the spectrum of adsorbed CO species. Since the metal–carbon vibration is out of the range of IR transmittance, the intense C–O bond vibrational frequency can provide information about the adsorbate–surface interaction. The blue shift observed on higher-valence doped catalysts indicates that the Pt–CO bond is weak, resulting in a strong C–O bond which manifests itself in a shift of CO vibrational frequencies to higher values approaching that of free CO (2143 cm^{-1}). A similar shift in the frequency of CO adsorption has been reported by Vannice *et al.* (*9*) over Pt/TiO_2

catalysts in the SMSI state. These authors reported the HF band to occur at 2050 cm^{-1} on normal Pt/TiO_2 and at 2070 or 2080 cm^{-1} on Pt/TiO_2 in the SMSI state. This observation, in combination with results of this study, supports recent theories that in addition to the geometric factor, an electronic factor is also operative in the SMSI state.

The binding of CO to a metal surface occurs through formation of a σ bond by overlap of an empty d orbital ($d_{x^2-y^2}$) and a lone pair on the carbon atom of CO, and formation of a π bond between a filled metal d orbital (d_{xy}) and an empty antibonding π orbital (π^*) of CO. Then, if transfer of electrons from the doped carrier to the supported Pt particles is assumed to partially fill the empty Pt d orbitals of the surface atoms, the overlapping of empty Pt d orbitals ($d_{x^2-y^2}$) and a lone electron pair on the C atom will be less effective in forming a Pt–CO bond. On the other hand, the ability of filled d orbitals (d_{xy}) to backdonate electrons to the $2\pi^*$ orbitals of adsorbed CO will be enhanced due to greater availability of electrons. Nevertheless, donation of electrons to the $2\pi^*$ orbitals of CO cannot occur without the first step (formation of the σ bond) of the adsorption process. The first step is prevented by the unavailability of empty Pt d orbitals. Thus, the binding of CO to Pt atoms with saturated d orbitals is a difficult process as evidenced by suppressed and weaker chemisorption.

No frequency shifts are observed on Pt supported on lower-valence doped carriers. This phenomenon is due to the fact that electron transfer from Pt particles to the support requires a "hopping" mechanism from one acceptor site to another, which is a difficult process. Thus, in this case, no changes are observed in the CO adsorption spectrum and, in general, in the chemisorptive and catalytic properties of the supported metal.

The shift of the CO vibrational frequency is in the range 15–22 cm^{-1} for the 0.5% Pt catalysts supported on higher-valence doped TiO_2, while only 7–8 cm^{-1} for the 2% Pt catalysts. It may be recalled that CO stretching vibrational frequency decreases as CO coverage decreases owing to a reduction in dipole–dipole coupling (*20, 21*). Furthermore, the doped catalysts exhibit reduced saturation coverages. Thus, undoped platinized titania with the same CO coverage as doped catalysts would yield a CO vibrational frequency lower than 2057 cm^{-1}. The value obtained from a plot of CO stretching frequency versus CO coverage for Pt/Al_2O_3 (*16*) and Pt/SiO_2 (*10*) is approximately 30 cm^{-1}/100% CO coverage. This is the difference in shifts of CO stretching frequency between a fully CO-covered surface and an isolated CO molecule with no dipole–dipole interactions. If this value is assumed also to apply for platinized titania, the increase in the CO stretching vibrational frequency is estimated to be in the range 35–40 cm^{-1} for the 0.5% Pt catalysts while only about 10 cm^{-1} for the 2% Pt catalysts. This difference is in accordance with chemisorption studies which have shown that reduction of the chemisorption capacity of low-metal-content catalysts (high dispersion) is significantly more pronounced than that of higher-metal-content (low dispersion) catalysts. The suppression factor for H_2, O_2, and CO chemisorption capacity is approximately 80% on 0.5% Pt catalysts while only 20–30% on 2% Pt catalysts. This is due to the fact that charge transferred into large metal crystallites is not as effective in altering the electron structure of surface metal atoms as charge transferred into smaller metal particles. Further discussion on the subject has been provided in Ref. (*1*).

(*d*) *Some Theoretical Considerations*

The model used to interpret results of this study is based on the theory of metal–semiconductor contacts (Schottky junctions). According to this theory the Fermi energy levels of a metal and a semiconductor in contact and at thermodynamic equilibrium are at equal heights. This re-

quirement results in electron transfer between the two solids, the direction of which depends on the initial (before contact) work functions of the two solids. Before accepting this theory as an explanation for the phenomena observed in this investigation, all other possible explanations must be carefully considered. Incomplete reduction of the metal, which could explain some of the observations made, was experimentally eliminated by varying reduction temperature between 200 and 300°C and reduction time between 2 and 10 h. No changes in hydrogen uptake were detected, indicating that the reduction of the metal was probably complete in all cases. Furthermore, Huizinga *et al.* (*24*) in TPR experiments under significantly milder conditions (5% H_2, linearly increasing temperature between 273 and 473 K at a rate of 5 K/min) have shown 75% reduction of the metal. This result is a strong indication that 100% of the metal was reduced under the severe conditions employed in this study.

Most of the observations made in this study could also be explained in terms of the conventional explanation for SMSI, namely that the metal becomes contaminated by some species emanating from the support. A number of arguments against this hypothesis, based on ESCA and other measurements, were provided in (*1*). It must also be added that this hypothesis cannot explain the observed shifts in CO stretching frequencies or the enhanced hydrogenation activity of Rh/TiO_2 (W) observed by Solymosi (*4*). To further test this hypothesis, TiO_2 was mixed with Wo_3 and heated at 500°C, instead of at the 900°C required for doping. At this temperature the foreign cation cannot diffuse into the crystal structure of TiO_2. No changes in the chemisorptive and catalytic properties of Pt supported on this material were observed. This is a strong indication that species diffusing from the support do not contaminate the metal surface. The work of Lane and Wolf (25), which has shown that induction of SMSI is more difficult when titania is in the rutile form (as in this study) than in the anatase form, provides an additional argument against this hypothesis.

Another criticism of the electron transfer theory, as applied to interpret alterations of chemisorptive and catalytic properties of metal particles supported on semiconducting carriers, is that metals have a high concentration of free electrons and only minimal perturbations of their electron state can be expected as a result of electronic interactions at the metal–semiconductor interface. We addressed this issue in an earlier publication (*1*) and showed that the difference in "affected volume" between the semiconductor and the metal is of the same order of magnitude as the difference in electron concentration between the two solids. Specifically, when the case of 0.5% Pt on TiO_2 doped with 0.1119 at.% W was examined, it was shown that the depletion region of the semiconductor at 300 K is a hemispherical volume of 640 Å radius.

These calculations can be extended a step further to obtain an order of magnitude estimate of the number of electrons transferred into the Pt particles per metal atom. Let us consider an isolated hemispherical Pt particle, 20 Å in diameter, in contact with an infinitely extending TiO_2 surface as shown in Fig. 8. The volume of the semiconductor which is partially depleted of electrons is a cylindrical volume of radius equal to the radius of the metal particle and a hemispherical volume of 640 Å radius. The volume of the former is negligible compared to that of the latter and thus it can be ignored. (This is equivalent to assuming that the metal particle is a point on the sur-

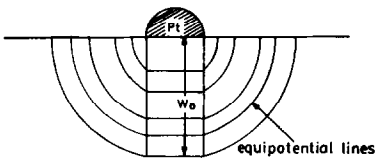

FIG. 8. Geometric model used in estimation of charge transferred into Pt particles.

face and the semiconductor volume partially depleted of electrons is a hemispherical volume of 640 Å radius.)

The potential distribution in the depletion region of the Schottky barrier can be estimated by solution of the one-dimensional Poisson equation under the depletion approximation (*26, 27*)

$$(d^2V/dr^2) = -4\pi qN_d/\varepsilon_s, \quad 0 < r < W_0, \quad (2)$$

where $V(r)$ is the potential distribution, q is the electron charge, ε_s is the permittivity of the semiconductor, N_d is the donor electron concentration, and W_0 is the radius of the affected hemispherical volume. Using the boundary conditions

$$(dV/dr) = V = 0 \quad \text{at } r = W_0 \quad (3)$$

the following expression for V as a function of r is obtained:

$$V(r) = -[2\pi qN_d/\varepsilon_s]W_0^2[1 - r/W_0]^2. \quad (4)$$

In the derivation it is assumed that all donors are fully ionized. However, at low temperatures this is not the case and the concentration of free electrons, n_0, may be substituted for N_d.

The concentration of electrons at any point, r, within the depletion region is given by (*27*)

$$n(r) = n_0 \exp[qV(r)/k_BT], \quad (5)$$

where K_B is Boltzmann's constant and T the absolute temperature. Substituting Eq. (4) into Eq. (5),

$$n(r) = n_0 \exp[-(2\pi q^2 n_0 W_0^2/\varepsilon_s k_B T) \times (1 - r/W_0)^2]. \quad (6)$$

Equation (6) shows the electron concentration profile within the depletion region of the semiconductor. The difference in total number of electrons within the same volume before and after contact of the metal with the semiconductor designates the number of electrons transferred into the metal particle, n_t. Thus,

$$n_t = (2/3)\pi W_0^3 n_0 - \int_0^{W_0} 2\pi r^2 n(r)dr. \quad (7)$$

Equation (7) can be solved numerically to determine n_t. Values of all parameters involved were estimated and reported in a previous publication (*1*).

A hemispherical Pt particle, 20 Å in diameter, contains approximately 140 atoms. Most of these atoms are either free surface atoms or atoms at the metal–support interface. Therefore, almost all of them will be affected by charge transferred into the particle. The charge transferred per metal atom was estimated, by numerical integration of Eq. (7), to be approximately one electron per metal atom. This value is of course very high, primarily due to the geometric model which was employed for its estimation. It was assumed that a Pt particle exists *isolated* on a circular area of 640 Å in radius (not counting the area of the particle itself). This, of course, is not true. It is estimated that in such an area there would be approximately 200 Pt particles. All these particles will interact in a similar manner with the doped carrier. The potential distribution and electron concentration profiles within the semiconductor will be affected by these interactions. Thus, the magnitude of charge transferred into the isolated Pt particle estimated in this manner should be considered only as an upper limit. A lower limit can also be estimated if it is assumed that in the same area of 640 Å radius there exists a single Pt particle of volume and contact area equal to the sum of volumes and contact areas of the 200 particles. This results in a particle of 140 Å radius, consisting of approximately 28,000 atoms. The thickness of this particle is not important since we will again assume that all atoms are equally affected by electronic interactions at the metal–semiconductor interface.

The number of electrons transferred into this particle per atom of Pt was estimated in a manner identical to that used previously and it was found to be 0.008 electron per Pt atom. This represents the lower limit in the number of electrons transferred into the metal particles per atom of Pt.

The actual magnitude of charge trans-

ferred lies between these two limits and it is probably closer to the upper limit since the geometry employed to estimate the lower limit is totally unrealistic. In any event, these estimates indicate that the charge transferred into small metal crystallites in contact with semiconducting supports could be significant enough to alter chemisorptive and catalytic properties of surface metal atoms. They also show that charge transferred per metal atom is a strong function of the size of metal crystallites as well as metal content of the catalyst which defines the surface density of the crystallites. These factors become even more important if it is realized that the charge transferred is distributed in a small distance into the metal particles (Thomas–Fermi screening distance) and surface atoms for electrostatic reasons. These considerations are reflected in the results of this investigation which show that the magnitude of alteration of surface properties is a strong function of metal content and metal crystallite size, decreasing dramatically with increasing particle size and metal content.

CONCLUSIONS

The following conclusions can be drawn from the results of this study:

(i) Altervalent ion doping of titania has a significant influence on its specific electrical conductivity and activation energy of electron conduction. This is indirect evidence that the Fermi energy level is also significantly affected by the doping process. Incorporation of cations of higher valence into the crystal structure of TiO_2 results in an increased Fermi level due to increased concentration of free electrons. Electrical conductivity of platinized titania is a strong function of the environment in which the sample exists.

(ii) The CO chemisorption capacity of higher-valence doped platinized titania is reduced, probably due to electronic interactions at the metal–support interface which result in electron transfer from the semiconducting support to the Pt crystallites.

(iii) A blue shift observed in the CO adsorption frequency, indicating weakened chemisorption of CO on Pt supported on higher-valence doped carriers, probably originates from higher saturation of Pt *d* orbitals.

(iv) Order of magnitude estimation of charge transferred into Pt crystallites indicates that the amount of charge transferred per metal atom can be significant and it depends on metal dispersion as well as metal content of the catalysts, as it defines the surface density of supported Pt particles.

REFERENCES

1. Akubuiro, E. C., and Verykios, X. E., *J. Catal.* **103,** 320 (1987).
2. Schwab, G.-M., "Advances in Catalysis" (D. D. Eley, P. W. Selwood, and P. B. Weisz, Eds.), Vol. 27, p. 1. Academic Press, San Diego, 1978.
3. Solymosi, F., *Catal. Rev.* **1,** 233 (1967).
4. Solymosi, F., Tombacz, I., and Koszta, J., *J. Catal.* **95,** 578 (1985).
5. Herrmann, J. M., and Pitchat, P., *J. Catal.* **78,** 425 (1982).
6. Solymosi, F., *in* "Contact Catalysis" (Z. G. Szabo and D. Kallo, Eds.), Vol. 2, p. 204. Elsevier, Amsterdam, 1976.
7. Herrmann, J. M., *J. Catal.* **89,** 404 (1984).
8. Akubuiro, E. C., Ph.D. dissertation, Drexel University, Philadelphia, PA, 1986.
9. Vannice, M. A., Twu, C. C., and Moon, S. H., *J. Catal.* **79,** 70 (1983).
10. Stoop, F., Toolenaar, F. J., and Ponec, V., *J. Catal.* **73,** 50 (1982).
11. Sheppard, N., and Nguyen, T. T., *in* "Advances in Infrared and Raman Spectroscopy" (R. J. Clark and R. E. Hester, Eds.), Vol. 5. Hayden, London, 1978.
12. Froitzheim, H., Hopster, H., Ibach, H., and Lehwold, S., *Appl. Phys.* **13,** 147 (1977).
13. Ibach, H., *Surf. Sci.* **66,** 56 (1977).
14. Tanake, K., and White, J. M., *J. Catal.* **79,** 81 (1984).
15. Bashard, Y., Zhou, X., and Gulari, E., *J. Catal.* **94,** 128 (1985).
16. Primet, M., *J. Catal.* **88,** 273 (1984).
17. Primet, M., Baset, J. M., Mathieu, M. V., and Prettre, M., *J. Catal.* **29,** 213 (1973).
18. Goodwin, J. G., and Naccache, C., *J. Catal.* **64,** 482 (1980).

19. Yates, J. T., Duncan, T. M., Worley, S. D., and Vaughan, R. W., *J. Chem. Phys.* **70,** 1219 (1979).
20. Crossley, A., and King, D. A., *Surf. Sci.* **68,** 528 (1977).
21. Hoffman, F. M., and Bradshaw, A. M., *J. Catal.* **44,** 328 (1976).
22. Shigeishi, A., and King, D. A., *Surf. Sci.* **58,** 379 (1976).
23. Barth, R., Pitchai, R., Anderson, R. L., and Verykios, X. E., submitted for publication.
24. Huizinga, T., van Grondelle, J., and Prins, R., *Appl. Catal.* **10,** 199 (1984).
25. Lane, G. S., and Wolf, E. E., *J. Catal.* **105,** 386 (1987).
26. Dalven, R., "Introduction to Applied Solid State Physics." Plenum, New York, 1980.
27. Tyagi, M. S., *in* "Metal–Semiconductor Schottky Barrier Junctions and Their Applications" (B. L. Sharma, Ed.). Plenum, New York, 1984.